- Technical Paper -

SHEAR FATIGUE PERFORMANCE AND CRACK SURFACE OBSERVATIONS IN PVA-ECC BEAMS WITHOUT WEB REINFORCEMENT

Benny SURYANTO[*1], Mahyarudin DALIMUNTHE[*2], Kohei NAGAI[*3] and Koichi MAEKAWA[*4]

ABSTRACT

This paper describes the results of fatigue tests on three shear ECC beams without web reinforcement. Shear fatigue is found to be more severe than bending fatigue, with fatigue life of approximately one to two orders lower. While the crack surface of control beam tested in static are rough and hairy, those tested in fatigue are all smooth. The damage at cracks around the web region is much more extensive than those nearby loading and support points. At the web region, fibers were completely worn off, while at other regions they bent down and deformed permanently along the crack surfaces.

Keywords: shear fatigue, reduced fatigue life, fiber damage, smooth crack

1. INTRODUCTION

ECC is designed to exhibit multiple cracks under service loading [1]. As a consequence of externally applied loads or ambient environments, cracks in a structural ECC component are exposed to repetitive loading. When a repeated load is severe enough to trigger fatigue damage, damage rapidly accumulates and can lead to premature deterioration or even unexpected failure. Fatigue life assessment is, therefore, of particular important in structural ECC components that are exposed to high repetitive loading such in recent ECC applications as bridge decks, link slabs, and patch pavement repairs [2,3].

Fatigue life of ECC is typically represented by empirically derived equations based on small-scale specimens. Matsumoto *et al* performed extensive flexural fatigue tests on prism ECC specimens having a cross section of 100×100 mm^2 [4]. They revealed that the S-N curve of ECC resembled those of metallic materials and could be approximated with a bilinear relation. They found that the fatigue life was dependent on the stress magnitude, which also dictated the numbers of multiple cracks. Qian *et al* demonstrated that ECC prisms of 50×76 mm^2 and ECC overlay 25 mm cast on two concrete substrates exhibit excellent fatigue performance of at least nine orders of magnitude higher than that of concrete overlay [5,6].

Although it becomes more common to conduct flexural fatigue tests, it should be noted that such a test does not actually replicate the behavior of multiple cracks in actual structures for several reasons. In flexural test, ECC exhibits multiple cracks that alternately open and close. In actual structures, cracks can undergo mixed mode deformations, including opening, closing, and slippage. That is, flexural fatigue test fails to replicate rubbing/slippage of crack surfaces, which can accelerate damage the fibers at cracks. Another reason is that complete crack closure does not occur in a laboratory fatigue test since the minimum load is usually kept about 10-20% of the applied load. Matsumoto *et al* demonstrated that the closure of cracks, in fact, accelerated damage and introduced faster rate of fiber bridging degradation in ECC by one to two orders of life [7].

Shear beam fatigue test imposes a good opportunity to study the behavior of multiple cracks in ECC during the material strain-hardening. In such a test, diagonal shear, multiple cracks are exposed to alternate opening and closing, and shearing. Under repetitive loading, the crack surfaces and the fibers bridging them can be damaged. Interactions between these complex behaviors can be thus evaluated.

This paper reports an ongoing experimental program that is undertaken for assessing shear fatigue performance of PVA-ECC. This research program involves one shear beam subjected to a monotonic point load at midspan and three shear beams subjected to a stationary pulsating load at midspan with varying magnitudes. Assessment is made to the fatigue life, cracking behaviors, failure modes, and conditions of crack surfaces and fibers along diagonal shear cracks.

2. EXPERIMETAL PROGRAMS

2.1 Test beams

This experimental program involves the testing of four shear-critical ECC beams. The beams were of similar dimensions of 100×225×1,400 mm and were reinforced with four 16-mm-threaded deformed bars. In a span of 1,300 mm, all beams were each subjected to point load applied at midspan. Details of the test beams are shown in Fig. 1.

*1 Postdoctoral research fellow, Dept. of Civil Engineering, University of Tokyo, Ph.d, JCI Member
*2 Graduate student, Dept. of Civil Engineering, University of Tokyo, B.E., JCI Member
*3 Lecturer, Dept. of Civil Engineering, University of Tokyo, Dr. E., JCI Member
*4 Professor, Dept. of Civil Engineering, University of Tokyo, Dr. E., JCI Member

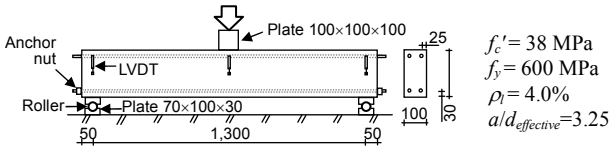

Fig.1 Details of test beam

Table 1 Summary of experimental program

ID	Loading type	P_{max} $\%P_{static}$	P_{min} $\%P_{max}$	Start dayth	Finish dayth
BS	Static	-	-	28	28
BF85	Fatigue	85	12.5	28	28
BF60	Fatigue	60	12.5	29	29
BF50	Fatigue	50	12.5	29	36

2.2 Material and Fabrication

A premixed Engineered Cementitious Composite (ECC) [1], which contained 2% of PVA fibers by volume, was used to cast the test beams. The mix proportion of the PVA-ECC is shown in Table 2.

In each casting, the PVA-ECC was mixed for ten minutes. After mixing, the fresh ECC was poured to steel frameworks, which had been oiled. The surface of the ECC was smoothened with a trowel and then covered with a plastic sheet. The average slump flow and air content of the PVA-ECC was 535 mm and 11%, for the first batch, and 520 mm and 13 %, for the second batch. The average density was 1,830 kg/m^3.

After two days, the beams were demolded and wrapped with wet clothes and plastic sheets. The average compressive strength from three 100×200 mm cylinders were 37 MPa at 28 days.

All reinforcements were threaded bar, with a nominal diameter of 16 mm. Table 3 lists the property of the rebar from three coupon tests.

Table 2 Mix Proportion of PVA-ECC [1]

W/(C+FA) (%)	Water (kg/m^3)	S/(C+FA) (%)	PVA Fibers (%), in vol.
42.2	350	70	2.0

Note: W: Water, C: Cement, FA: Fly Ash, S: Sand. PVA fibers: diameter is 0.04 mm, length is 12 mm, and tensile strength is 1,600 MPa.

Table 3 Reinforcement properties

D mm	A mm^2	f_y MPa	E_s GPa	Type
15.9	198.6	558	185	Threaded deformed bar

2.3 Test Procedure

Both static and fatigue loading tests were conducted on a 220 kN universal testing machine. The static test was displacement-controlled, while the fatigue test was load-controlled. The upper load level in the fatigue tests was set among 50, 60, and 85% of the ultimate capacity of the beam tested in static loading. The lower load level was fixed at 12.5% of the upper load. Constant amplitude sinusoidal loading were applied at a frequency of 0.2 Hz, for Beams BF85 and BF60, and at 1.0 Hz for Beam BF50.

3. TEST OBSERVATIONS AND DISCUSSIONS

3.1 Static Test (Beam BS)

The static load deflection curve is shown in Fig. 2. The curve shows a pronounced curvature with two notable turning points. The first turning point corresponds to the first diagonal crack occurring at a load of approximately 20 kN. Since then, the curve is highly nonlinear, occurring due to the formation and propagation of diagonal shear-multiple cracks and few flexural cracks with increasing loading. The second turning point corresponds to the yielding of tensile reinforcements. The beam response thereafter is nearly flat. During this post-yielding stage, about five diagonal full-length shear cracks were visible, while other cracks were hardly seen. The beam finally failed in a brittle manner at a load of 134.8 kN due to the penetration of a single diagonal crack to the upper surface of the beam next to the loading plate. Crack pattern of the beam after failure is shown in a later part of this paper for comparison with those observed from beams under fatigue loading.

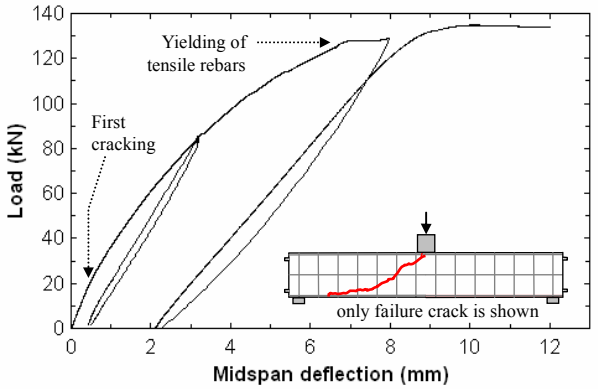

Fig.2 Load-deflection response of Beam BS under static loading

3.2 Fatigue Test (Beams BF85, BF60, and BF50)

(1) S-N Curves

The relationship between loading amplitude S and fatigue life N for the three beams is shown in Fig. 3. From this limited test data, it appears that the S-N curve for PVA-ECC under shear fatigue decreases linearly with log of the number of cycles. The S-N curve does not to converge to the ordinate of S at a value of 1.0. Fatigue limit, if such exists, has not been observed.

Plotted also in Figure 3 are S-N curves for PVA-ECC under flexural loading by Matsumoto *et al* [4] and Qian *et al* [5]. The comparison indicates that shear fatigue results in a more rapid breakdown in the properties of the PVA-ECC than does flexural fatigue. It also indicates that the S-N curve for shear fatigue is in a comparable slope to that from Reference [4] and approximately one to one-and-a-half orders lower. Compared to the data from Reference [5], the shear fatigue life is one order lower at S 0.8 and more than two orders lower at S lower than 0.7.

Figure 3 also shows two S-N curves for concrete. The first curve relates to shear fatigue for concrete beam without web reinforcement proposed by Ueda [8].

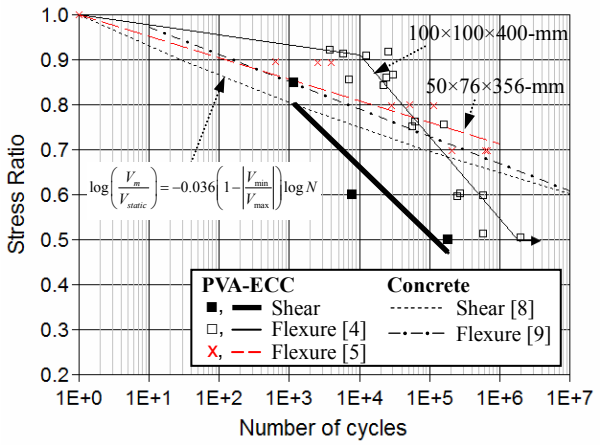

Fig.3 Shear fatigue life of PVA-ECC under three different constant load amplitudes

The load amplitude V_{min}/V_{max} is set at 0.125. The second curve relates to flexural fatigue for plain concrete, averaged from eight experiments by Lee and Barr [9].

With respect to the stress amplitude S, PVA-ECC appears to exhibit a better fatigue performance than concrete at higher stress amplitudes than 0.8 (shear) and 0.75 (flexure), and worst at lower stress amplitudes. The indication is that lower stress amplitudes are associated with a large number of cycles and crack reversals that introduce more damage to the PVA-ECC.

Considering the different material types, it is observed in Fig. 3 that while flexural and shear fatigue in concrete is somewhat identical, they differ quite significantly in PVA-ECC. In concrete, both flexural and shear fatigue generally depend on the rate of crack propagation. The similarity suggests that the rate, which is generally dictated by the area of concrete being compressed above the propagated crack, is comparable. To investigate the mechanisms of shear fatigue in PVA-ECC, next sections focus on the response and the cracks developed in the test beams.

(2) Deflection, Crack Patterns, and Failure Modes

The progress of the midspan deflection of each beam is shown in Fig. 4. It appears that higher load levels result in larger deflection amplitudes. The midspan deflection steadily increases and, when reaches a certain value, rapidly increases. The rate of the acceleration is notably different due to variation of the angle of diagonal shear cracks next to loading plate.

All the three beams exhibited cracking in a very similar way. Figure 5 shows the development of visible cracks in Beam BF50 during the first 100K cycles. Initially, diagonal shear multiple cracks formed, but they were hardly visible. Under repeated loading, these cracks alternately opened, closed, and slip. After approximately 80, 600, and 5K cycles (Beam BF85, BF60, and BF50, respectively), only two to four predominant diagonal shear cracks were visible at an angle of about 40 to 50° around the mid-high of each web region of each beam (see Note A in Fig. 5). The tip of these cracks then propagated towards support and loading plates as the loading further progressed (see Note B). The crack propagation to the loading plate occurred earlier, yet it was later arrested when it came close to the bottom of compression rebars (see Note C). The diagonal shear cracks, when propagated toward the support, merged with the pre-existing flexural cracks (see Note D). Where they merged, it was observed that the deformation was mainly carried by dowel of the two tensile rebars, particularly at the flexural crack D.

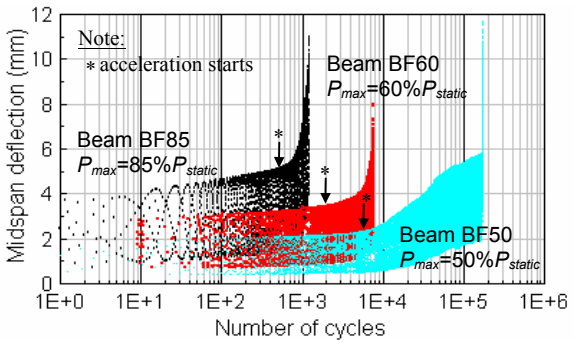

Fig.4 Deflection progress of the test beams

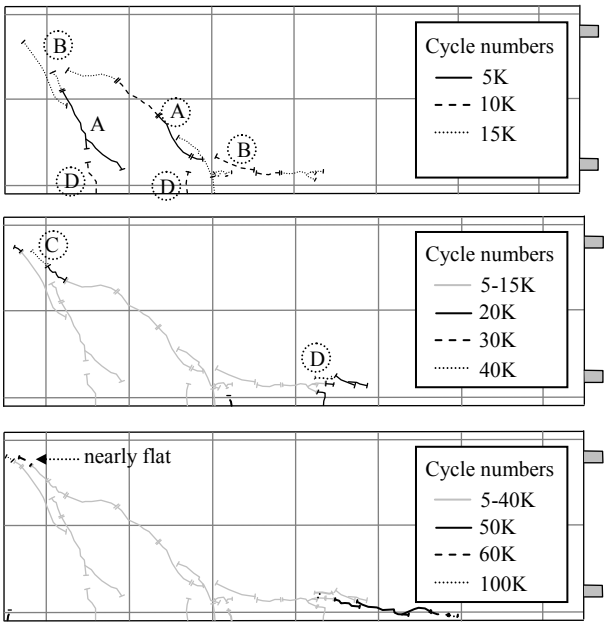

Fig.5 Development of visible cracks in Beam BF50

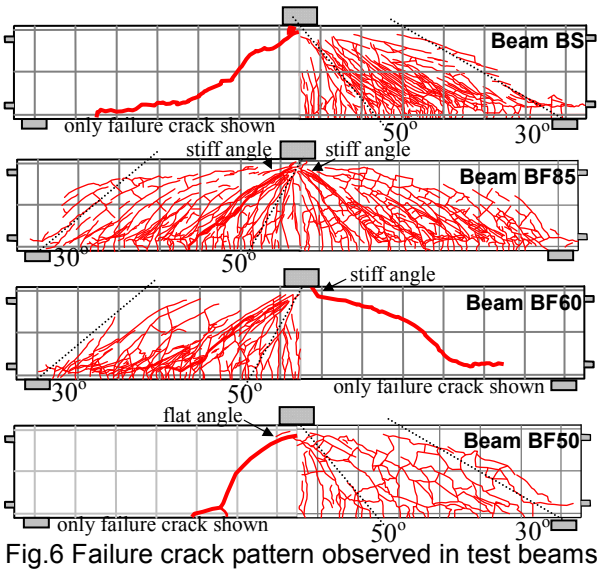

Fig.6 Failure crack pattern observed in test beams

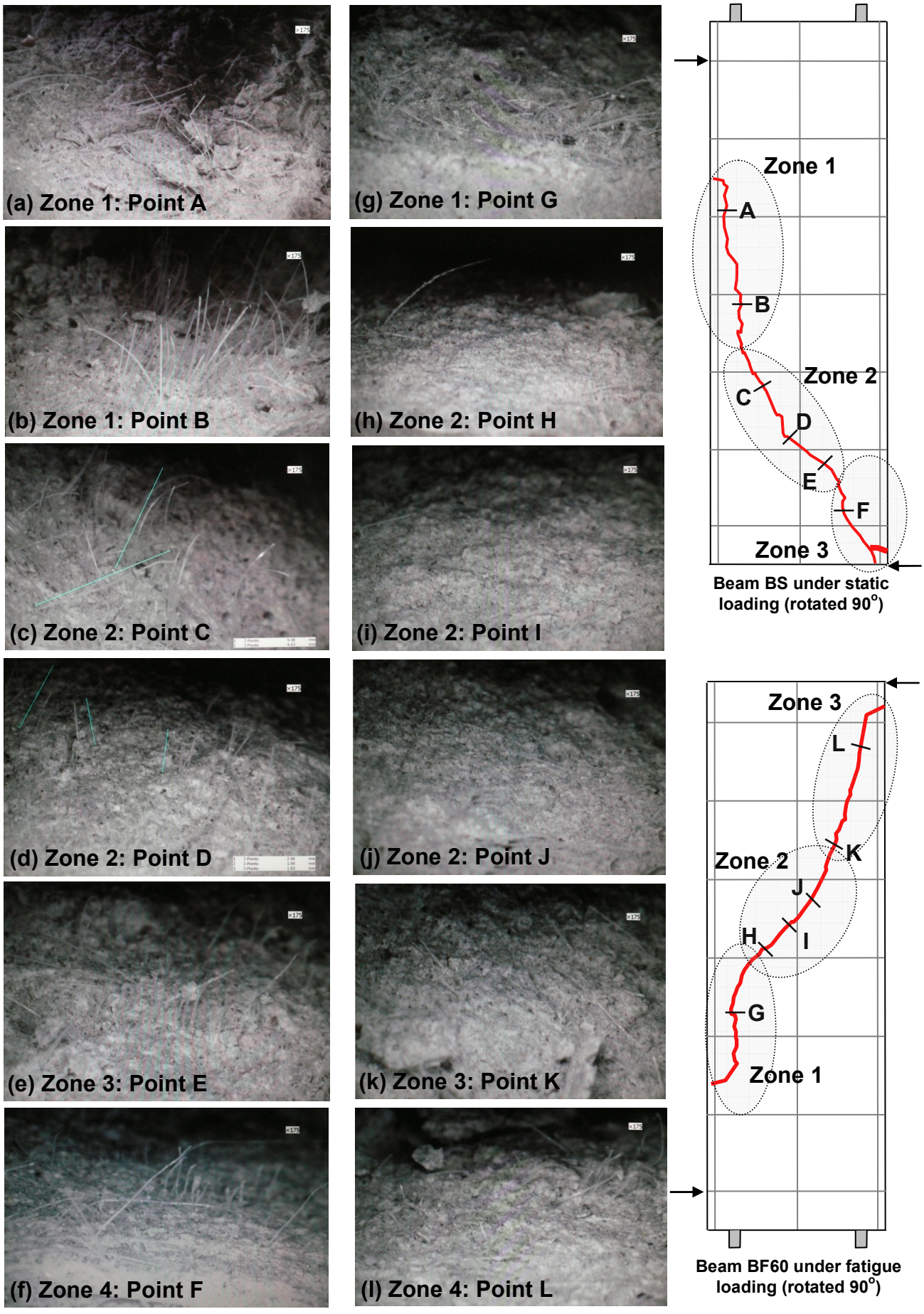

Fig.7 Failure crack surface in Beams BS and BF60 observed after testing and magnified 175 times

The failure of the Beams BF85 and BF60 were due to the penetration of one diagonal shear crack to the upper surface of the beam next to the loading plate (see Fig. 6). In Beam BF50, the tip of the diagonal crack when approached the loading plate was nearly flat. As a result, this beam tended to exhibit a longer fatigue life for this particular load level. Beam BF50 failed once the two diagonal shear cracks from both sides of the beam merged and one of the tensile rebars fractured.

Figure 5 shows the crack pattern of the test beams after failure. All beams exhibited diagonal shear cracks formed predominantly at angles of between 30^o and 50^o with respect to the longitudinal direction toward the loading point. In Beam BS, they were uniformly spaced at about 10 mm. The diagonal shear cracks in Beam BF85 distributed in a wider area, with a spacing of about 25 mm. The average crack spacing in Beam BF60 was about 30 mm. In all cases, the predominant shear crack formed at an angle of about 45^o. Overall, the number of diagonal shear crack decreased with decreasing load magnitude.

(3) Observations on the Failure Surfaces

To obtain a measure of the mechanisms of crack reversals in shear fatigue, the failure crack surface is compared in Fig. 7. Figure 7 (a) to (f) show the crack surfaces observed from Beam BS subjected to static loading, while Figure 7 (g) to (l) show those observed from Beam BF60 under fatigue loading; all photos shown were taken after testing.

In Beam BS, three typical qualities of surface were observed. For this reason, the surface is divided into three zones: namely, Zone 1, 2, and 3 (see Fig. 7). In Zone 1 [Points A and B in Fig. 7(a) and (b)], where the crack formed along the bottom flexural rebars, the surface was notably jagged and rough. Many protruding fibers were observed from the crack surface, with lengths varying between 1.5 and 5.0 mm. In Zone 2 [Points C to E in Fig. 7(c) to (e)], where the crack oriented at about 45^o, the surface was moderately rough. More fibers were observed at Points C and E, with lengths varied between 1.5 and 5.0 mm. At Point D [see Fig. 7(d)], most of the protruding fibers were less than 0.1 mm, and only a few were 1.5 to 2.5 mm long. This suggests that the fibers were ruptured when the crack width was small. The surface in Zone 3 [Point F in Fig. 7(f)] was little rougher than Zone 2, but much smoother than Zone 1. Fibers were apparently similar to those observed from Points C and E. All crack surfaces, when touched by a finger, were hairy and rough.

Beam BF60 subjected to fatigue loading exhibited much flatter and smoother crack surface than those observed in Beam BS [compare Fig. 7 (g) to (l) with Fig. 7 (a) to (f)]. The smoothest crack planes were observed along Points H to K, being the smoothest at Points I and J. This is expected since the diagonal cracks at Points I and J were inclined, such that they attempted to rub down each other during repeated loading.

Worse yet, rubbing of the two diagonal crack surfaces caused the fibers in Zone 2 in Beam BF60 almost completely worn off [see Fig. 7 (h) to (j)]. At Points G, K, L, several fibers were still observed. They appeared to completely bend down and permanently deformed along the crack surface. The indication was that the fibers at this location were initially pulled out [see those in Beam BS Zone 1 shown in Fig. 7(a) and (b), for instance], buckled and ruptured under loading cycles, and ultimately compressed in between the two crack surfaces during crack closure. It is believed that these fibers survived since the cracks at that location did open and close and did not extensively slide.

To gain deeper insights into the behavior of shear cracks, additional visual observations were made in Beam BF50 during repeated loading. Two scanned locations were determined, one at the mid-high of the beam, and the other one at the region nearby the bottom rebars.

Figure 8 (a) and (b) depicts the behavior of 5-mm long diagonal shear crack at the mid-high of the beam at 30K cycles. As one would expect, the crack was under mixed mode deformations. The crack open and slide under the maximum loading, with a maximum width of about 1 mm. Under the minimum loading, the two crack surfaces closed and rubbed over each other. Twelve PVA fibers were identified. Fibers 1, 3, 4, 5, 9 were bridging the two crack surface. Fibers 6, 7, 8, 10, 11, and 12 had already ruptured, while Fiber 2 had been pulled out because it was on the surface and hence should be neglected. All fibers were compressed and rubbed by the two crack surfaces during crack closure.

At 70K cycles [see Fig. 8(c) and (d)], it was observed that only Fibers 4, 5, 8, and 9 remained, and the crack did not completely close under the minimum loading. This suggests that there was a transition in the dominating shear fatigue damage. At low cycles, damage accumulated due to crack closure and slip that broke the fibers at diagonal shear cracks. At high load cycles, this mode did not contribute anymore and the damage is attributed by the propagation of cracks occurring at the tip of diagonal shear cracks nearby to the loading plate at midspan.

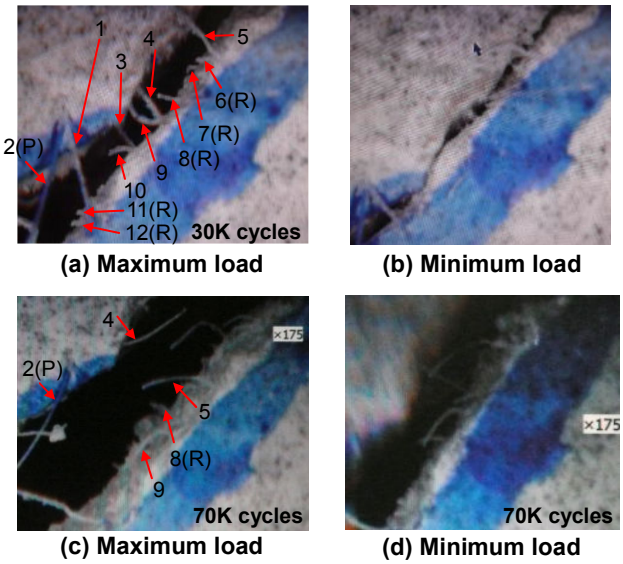

Fig.8 Diagonal shear crack response at (a), (b) 30K cycles, (c) and (d) 70K cycles

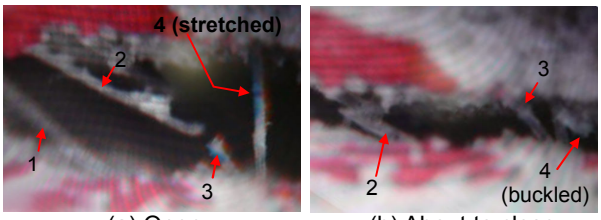

(a) Open (b) About to close

Fig.9 Crack behavior nearby the bottom tensile rebars at approximately 70K cycles

Figure 9 (a) and (b) show the behavior of one crack segment nearby the bottom rebar at 70K cycles. The cracks alternately opened and closed during repeated loading and apparently did not slide over each other. Four fibers were observed. Fibers 1 and 2 had pulled out from one-end and bent down along the crack surface. Fiber 3 had already ruptured. Fiber 4 survived, being stretched during crack opening and buckled during crack closure. This observation suggests that the bent fibers observed previously in Fig. 7 (g), (k), and (l) were those that experienced pulled out from one-end.

4. CONCLUSIONS

(1) S-N curve for PVA-ECC beams without web reinforcement appears to be linear in a semi-log plot at *S* ranging between 0.50 and 0.85. This line does not converge to *S* equals to 1.0. Fatigue limit is not observed within the range of *S* considered.

(2) S-N curve for PVA-ECC under shear fatigue exhibits a comparable slope to those under flexural fatigue reported by Matsumoto *et al* [4] and a stiffer slope of about twice to that reported by Qian *et al* [5]. At intermediate *S* amplitude of 0.7, *N* is approximately one order shorter to the former and two orders shorter to the later.

(3) Although the number of multiple cracks decreased with decreasing loading amplitude, the visible diagonal shear cracks appeared identical regardless the maximum load levels. It involved the formation of two to four predominant cracks at the web of the beam and their propagation to both support and loading plates. Failure occurred when the diagonal cracks propagated outward, adjacent to the loading plate, or merged with other diagonal cracks from another side of the beam. Failure was delayed when the tip of the diagonal crack nearby the loading plate was nearly flat.

(4) The surface of the failure cracks at the web region was smoother than that at regions nearby support and loading plates. While the surface of the failure cracks of the beam tested under static was rough and occasionally jagged, those under fatigue loading were all smooth and flat.

(5) It was found that the inclination of the failure crack surface significantly affected the fibers on the crack surface. Where the crack surface was about horizontal, many protruding fibers were observed of about 1.5 to 5 mm long. Inclined cracks around the beam web region had fibers about 0.1 mm, and a few were 1.5 to 2.5 mm.

(6) In Beams under fatigue loading, the fibers at the web region were almost completely worn off, underscoring the significance of repeated opening, closing, and rubbing of crack surfaces. At other locations, the fibers appeared to bend down along the crack surface, an indication of being compressed by two crack surfaces during repeated loading.

(7) The deterioration due to crack reversals along the diagonal shear cracks appeared to occur at an early stage, when the crack width was still small. The deterioration thereafter was contributed by those nearby the tip of the diagonal cracks.

ACKNOWLEDGEMENT

The first author acknowledges the fellowship from the Japan Society for the Promotion of Science (JSPS) that enables him to carry out this research at the University of Tokyo.

REFERENCES

[1] JSCE, “Recommendations for Design and Construction of HPFRCC,” Concrete Library 127, 2007, pp.129-135 (in Japanese).

[2] Kunieda, M., and Rokugo, K., “Recent Progress on HPFRCC in Japan—Required Performance and Applications,” Journal of ACT, V. 4, No. 1, 2006, pp. 19-33.

[3] Li, V. C., Lepech, M., and Li, M., “Field Demonstration of Durable Link Slabs for Jointless Bridge Decks Based on Strain-Hardening Cementitious Composites,” Michigan Department of Transportation Research Report RC-1471, 2005, 110 pp.

[4] Matsumoto, T., Suthiwarapirak, P., and Kanda, T., “Mechanisms of Multiple Cracking and Fracture of DFRCC under Fatigue Flexure,” Journal of ACT, Vol. 1 No. 3, 2003, pp. 299-306.

[5] Qian, S., Victor C. Li, Han Zhang, and Gregory A. Keolaian "Durable and Sustainable overlay with ECC", Proc. of 9th Int. Conference on Concrete Pavements, California, August 2008.

[6] Qian, S. and Victor C. Li "Durable Pavement with ECC", Proc. of 1st Int. Conference on Microstructure Related Durability of Cementitious Composites, China, October 2008.

[7] Matsumoto, T., Wangsiripaisal, K., Hayashikawa, T, and Hea, X. “Uniaxial Tension–compression Fatigue Behavior and Fiber Bridging Degradation of Strain Hardening Fiber Reinforced Cementitious Composites,” International Journal of Fatigue, V. 32, Issue 11, 2010, pp. 1812-1822.

[8] Ueda, T., and Okamura, H., “Fatigue Behavior of Reinforced Concrete Beams under Shear Force,” IABSE Colloquium, Laussanne, 1982, pp. 415-422.

[9] Lee, M.K., and Barr, B. I. G., “An overview of the Fatigue Behaviour of Plain and Fibre Reinforced Concrete,” Cement and Concrete Composites, V. 26, Issue 4, 2004, pp. 299-305.